

# Journal of Photonics for Energy

PhotonicsforEnergy.SPIEDigitalLibrary.org

## Significance of light-soaking effect in proper analysis of degradation dynamics of organic solar cells

Michał Dusza  
Wiesław Strek  
Filip Granek

**SPIE.**

Michał Dusza, Wiesław Strek, Filip Granek, "Significance of light-soaking effect in proper analysis of degradation dynamics of organic solar cells," *J. Photon. Energy* **6**(3), 035503 (2016), doi: 10.1117/1.JPE.6.035503.

# Significance of light-soaking effect in proper analysis of degradation dynamics of organic solar cells

Michał Dusza,<sup>a,b</sup> Wiesław Streck,<sup>b</sup> and Filip Granek<sup>a,\*</sup>

<sup>a</sup>Wrocław Research Centre EIT+, Stabłowicka 147, Wrocław 54-066, Poland

<sup>b</sup>Institute of Low Temperature and Structure Research, Polish Academy of Science, Okólna 2, Wrocław 50-422, Poland

**Abstract.** One of the issues in the organic solar-cell technology that needs attention before mass production is its low long-term stability. These devices need often to be exposed to the light to improve their photovoltaic properties. This effect, known as light soaking, is the cause of challenges related to correct measurements and proper determination of the device lifetime. Lifetime determination and investigation of failure mechanisms of solar-cell devices require reliable measurement approaches. This paper presents the systematic studies on proper analysis of degradation dynamics of organic solar cells (OSCs) taking into account the light-soaking effect. Five groups of organic solar-cell annealed at various conditions (110°C to 170°C and nonannealed) were under investigation for 100 days. Measurement procedure for proper investigation of light-soaking effect is proposed. Solar-cell efficiency improvement, due to light-soaking effect, in range 8% to 27% was observed for as fabricated devices. After 100 days of study, the light soaking-related efficiency improvement increased up to over 100% of initial efficiency. Device lifetimes strongly depend on measurement methods, which were applied. Our results show the importance of taking into account the changes in magnitude of the light-soaking effect in measurements and degradation studies of OSCs. © The Authors. Published by SPIE under a Creative Commons Attribution 3.0 Unported License. Distribution or reproduction of this work in whole or in part requires full attribution of the original publication, including its DOI. [DOI: [10.1117/1.JPE.6.035503](https://doi.org/10.1117/1.JPE.6.035503)]

**Keywords:** degradation; lifetime; light soaking; organic photovoltaics; polymer solar cells.

Paper 16055 received May 9, 2016; accepted for publication Aug. 8, 2016; published online Aug. 26, 2016.

## 1 Introduction

Solution-processed organic solar cells (OSCs) have gained serious attention in the past few years due to unique advantages as follows: low-cost, high throughput roll-to-roll production, semi-transparency, lightweight, and flexibility.<sup>1-10</sup> Bulk-heterojunction solution-processed OSC with certified efficiency up to 9.57% was achieved.<sup>11</sup> However, limited stability of OSCs needs to be improved for outdoor applications.<sup>12-14</sup> Inverted OSCs provide better stability compared to conventional structure, due to following modifications: replace the Al metal contact with Ag metal contact to prevent oxidation and remove PEDOT:PSS away from the indium tin-oxide (ITO) surface to prevent etching of ITO.<sup>15-18</sup>

In most of the inverted solar-cell structures, metal-oxide layers (TiO<sub>2</sub> and ZnO) are used as an electron-transport layer (ETL). In both cases, the fabricated solar cells need to be exposed to light for a certain time to achieve their maximum photovoltaic properties.<sup>19</sup> This phenomenon, known as a light soaking (LS), occurs in the as-prepared solar cells, which exhibit low short-circuit current ( $J_{sc}$ ) and a kink shape (or S-shape) of  $I-V$  curve and thus low fill factor (FF).<sup>20,21</sup> There are two main mechanisms behind the light-soaking effect. In the first case, the filling of trap states upon illumination decreases the work function of the ETL, which reduces the potential barrier and thus improves the extraction of electron through the ITO/metal-oxide interface.<sup>19,22</sup> In the second case, the key role in the light-soaking effect plays the interfacial

\*Address all correspondence to: Filip Granek, E-mail: [filip.granek@gmail.com](mailto:filip.granek@gmail.com)

dipole between the metal-oxide/organic interface.<sup>23–25</sup> Sometimes the devices should be stimulated under solar simulator for at least few minutes ( $\sim 10$  min) at the  $1000\text{-W/m}^2$  illumination intensity, for saturation of their photovoltaic properties. For the outdoor application, this illumination time could be equal to 1 to 2 h per day due to much lower solar irradiation intensity each morning.<sup>19,26</sup>

Improvement of the stability of OSCs is crucial for their industrial applications, thus the proper methods to determine the stability that takes light-soaking effect into account should be considered. Stability testing International Summit on OPV Stability (ISOS) protocols for OSCs proposed by the ISOS committee describe both indoor and outdoor procedures for testing the solar cells.<sup>27</sup> Here, we propose the testing procedure for OSCs, with the focus on analysis of light-soaking effect and its changes during the degradation period of the solar cells. In this paper, few key problems in reliable measurements and stability determination taking into account LS effect of inverted OSCs are presented. The measurement procedure used for the presented analysis of light-soaking effect, delivers information on the duration of light-soaking illumination for saturation of photovoltaic properties, photodegradation due to illumination used for LS, and the most important thing for degradation aspect, i.e., the variation of improvement due to light-soaking effect during the degradation time. Furthermore, these studies and analyses were performed for cells of varying quality and have been held for 100 days.

## 2 Experimental Section

### 2.1 Solar-Cell Fabrication

OSCs were fabricated in the inverted structure ITO/ZnO/P3HT:PCBM/MoO<sub>3</sub>/Ag (Fig. 1). Glass substrates covered by prepatterned ITO (Ossila) were cleaned in acetone and isopropanol, for 30 min each, using an ultrasonic bath. Zinc-oxide layers were spin-coated from ethanol ZnO nanoparticles dispersion (Sigma-Aldrich) and were annealed at 500°C in air. Poly(3-hexylthiophene-2,5-diyl) (P3HT, Sigma-Aldrich) and phenyl-C61-butyric acid methyl ester (PCBM, Sigma-Aldrich) at mass ratio 1:0.8 were dissolved in the 1,2-dichlorobenzene (60 mg/ml) by 4 h stirring at 60°C and 18-h aging of the solution at 40°C. The active layers were spin-coated at 1000 rpm under nitrogen atmosphere.

Four conditions of bulk-heterojunction (BHJ) preannealing (110°C, 130°C, 150°C, and 170°C for 30 min) were applied to obtain various qualities of solar cells. Fifth group of solar cells was nonannealed (NA). Overheating of P3HT:PCBM active layer leads to crystallization of PCBM.<sup>28–31</sup> Using an optical microscope (model Keyence VHX-1000), the surface of P3HT:PCBM layer was observed and even for 130°C small PCBM crystals were found [Fig. 2(c)], similar to these observed by Chang et al.<sup>29</sup> Large amount of relatively small crystals (few micrometers in size) was observed for samples annealed at 150°C [Fig. 2(d)]. The largest crystals, but a small amount of them, were observed for samples annealed at 170°C [Fig. 2(e)]. Crystal size is relatively large when compared to the active layer thickness of  $\sim 300$  nm. Thus, such a large size of PCBM crystals is expected to act as defects in the solar-cell structure. For NA and annealed at 110°C samples, the dust particles rather than PCBM crystals were observed.

Last two layers, i.e., MoO<sub>3</sub> ( $\sim 12$  nm) and silver electrodes ( $\sim 120$  nm) were thermally evaporated under vacuum of  $2 \times 10^{-6}$  mbar. Active area of fabricated inverted OSC was defined by intersection of electrodes and was equal  $4.5\text{ mm}^2$ . Samples were not encapsulated. Five groups (110°C, 130°C, 150°C, 170°C, NA) of solar cells with various quality of BHJ were fabricated

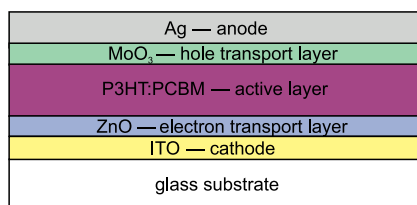
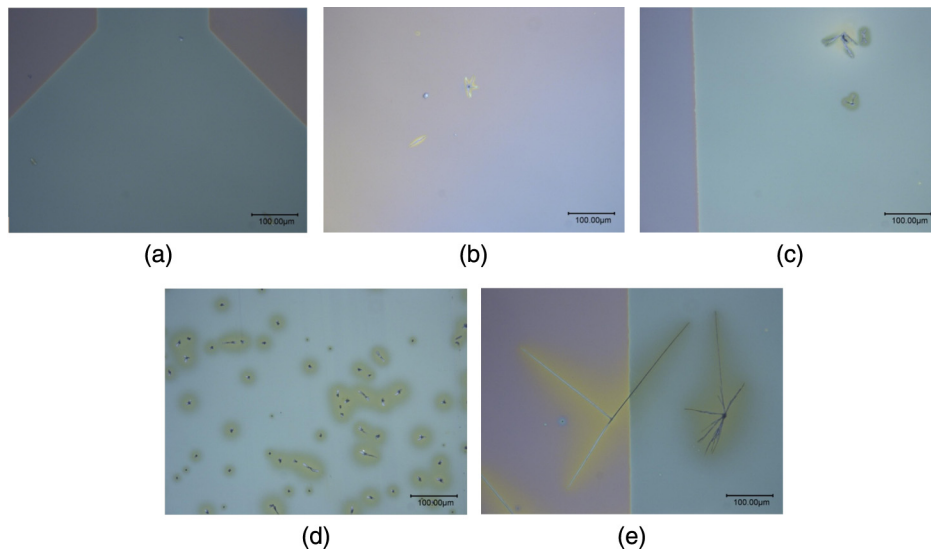


Fig. 1 Scheme of organic solar-cell stack.



**Fig. 2** Optical images of P3HT:PCBM surfaces (a) NA and annealed at various temperatures (b) 110°C, (c) 130°C, (d) 150°C, and (e) 170°C. Lines in the images (a), (c), and (e) show the edges of ITO/glass.

and were under investigation of light-soaking effect. Solar-cell properties measured in STC (Standard Test Conditions—spectrum AM1.5, 1000 W/m<sup>2</sup>, 25°C) using sun simulator (model #SS80AAA—Photo Emission Tech. and *I-V* Tracer Auxiliary Unit—PV Test Solutions) and Keithley 2401 Low-Voltage Source Meter were presented in Table 1.

**Table 1** As fabricated solar-cell properties (maximum, minimum, average, and standard deviation of  $\eta$ ,  $J_{sc}$ ,  $V_{oc}$ , FF) measured under standard test conditions (five to six solar cells per group).

Photovoltaic properties		Annealing temp.				NA
		110°C	130°C	150°C	170°C	
$\eta$ (%)	Maximum	1.80	1.86	1.50	1.13	0.95
	Minimum	1.53	1.45	1.18	1.00	0.69
	Average	1.65	1.69	1.34	1.06	0.78
	Std. dev.	0.12	0.20	0.15	0.05	0.09
$J_{sc}$ (mA/cm <sup>2</sup> )	Maximum	7.57	7.26	6.47	5.38	4.69
	Minimum	6.66	6.26	5.57	4.97	3.68
	Average	7.10	6.77	6.10	5.08	3.92
	Std. dev.	0.37	0.53	0.37	0.17	0.39
$V_{oc}$ (mV)	Maximum	598	605	591	583	564
	Minimum	585	587	561	551	510
	Average	592	598	575	566	554
	Std. dev.	5	8	15	15	8
FF (%)	Maximum	40.0	43.4	39.1	38.4	37.6
	Minimum	38.2	39.1	36.6	35.6	34.6
	Average	39.6	41.9	38.2	36.7	35.7
	Std. dev.	0.7	1.93	1.0	1.3	1.0

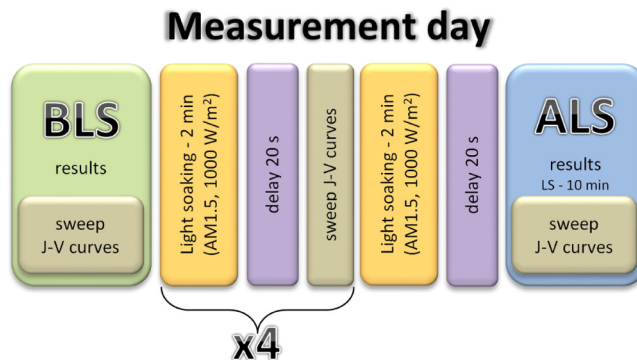


**Fig. 3** Light-soaking measurement procedure performed during every measurement day.

## 2.2 Light-Soaking Measurement Procedure

Study of the light-soaking effect is nontrivial, due to the heating of the cells during exposure to the illumination. To allow a proper interpretation of results, the following measurement procedure was applied. Six solar cells on each substrate were measured always in the same order under the same  $I$ - $V$  sweep conditions, such as direction of  $I$ - $V$  sweep scan from  $-1$  V (reverse bias) to  $+1$  V (forward bias) and scan rate  $1$  V/s. These conditions ensure the reliable scan of  $I$ - $V$  curve for fabricated OSCs. All samples were stored in the dark in the air atmosphere between the measurements. Between the  $I$ - $V$  sweeps of solar cells from one substrate, a 20-s delay was applied for cooling down the OSCs and on the other hand for cooling down the photodetector in solar simulator, which was used for the illumination intensity monitoring during the  $I$ - $V$  sweep.

During each measurement day the first measurement of the dark-stored sample was called “before light soaking” (BLS). After that OSCs were light soaked under solar simulator (AM 1.5 spectrum,  $1000$  W/m<sup>2</sup> irradiation) for 2 min. Next,  $I$ - $V$  curves sweeps were performed after 20 s delay (cooling-down as previous). This cycle procedure was repeated up-to 10 min of total light-soaking time. Last  $I$ - $V$  sweeps (after 10 min of LS) were called as “after light soaking” (ALS) (Fig. 3). Due to a large amount of data and for the clarity of reporting results, all photovoltaics parameters are presented as an average and standard deviations of five to six solar cells for each group.

## 3 Results

### 3.1 Improvements Due to Light-Soaking Effect

In Sec. 2, details of light-soaking measurement procedure were described. Due to various annealing conditions of OSCs, various properties of samples were obtained (efficiency in range from 0.69% up to 1.86%). LS improves the density of short-circuit current ( $J_{sc}$ ), FF, and the efficiency, while the open-circuit voltage ( $V_{oc}$ ) is constant. In Fig. 4, efficiencies of samples as a function of light-soaking time are presented as fabricated and aged solar cells.

After few minutes of illumination light-soaking effect is saturated for both as fabricated and aged samples. This is an evidence that total time of 10 min of LS is enough for saturation and proper analyses of LS in case of investigated solar cells. Higher photovoltaic properties were obtained for the samples annealed at low temperatures ( $110^{\circ}\text{C}$  and  $130^{\circ}\text{C}$ ) than for the overheated ( $150^{\circ}\text{C}$  and  $170^{\circ}\text{C}$ ) and the NA solar cells [see Figs. 4(a) and 4(b)]. During the first measurement day, relative efficiency improvement due to light-soaking effect was higher for the samples, which exhibit lower photovoltaic properties before being irradiated. It means that the lower the quality of the sample, the higher improvement due to LS could be expected.

### 3.2 Inspection of Light-Soaking Effect on Device Lifetime Determination

Device lifetime determination for OSCs is a key issue for proper analysis of degradation data. Difference of device lifetime determined from measurements before and after LS is significant. In Fig. 5, the solar-cell efficiency as a function of degradation time measured as BLS and ALS is

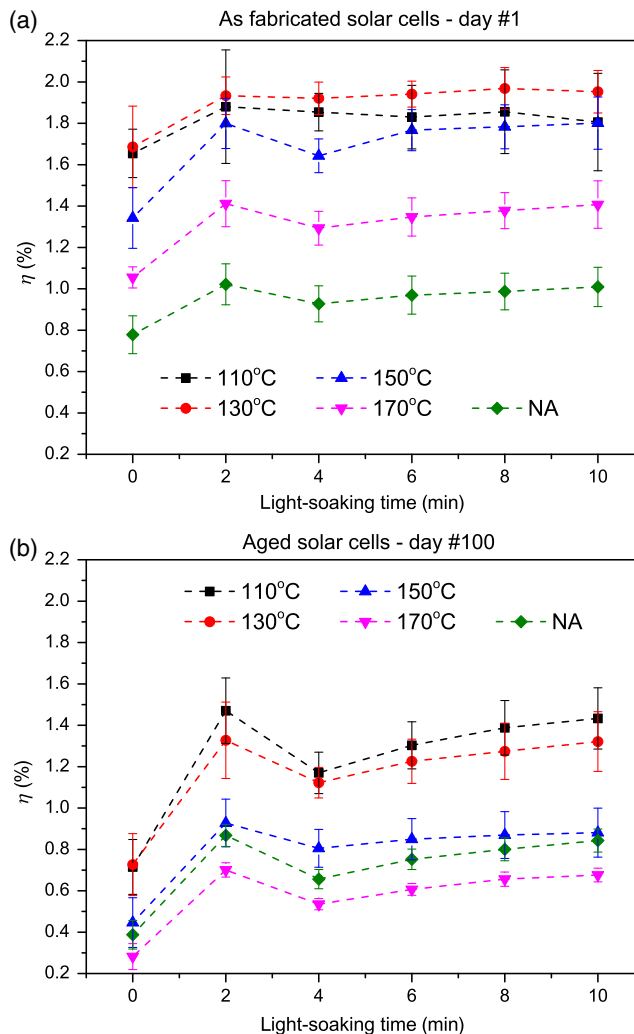


**Fig. 4** Efficiency as a function of light-soaking time for (a) fabricated and (b) aged OSCs annealed at various temperatures (each point is an average of five to six solar cells, dashed lines are guide to the eye).

presented. During the degradation decreasing of all photovoltaics parameters was observed and partial recovery of  $J_{sc}$ , FF, and efficiency was noticed due to light-soaking effect, while  $V_{oc}$  was constant. Lifetime is defined as a time after which the initial efficiency has fallen to 80% of this initial value ( $T_{80}$ ).<sup>27</sup> NA OSCs and annealed at low temperatures are more stable than these samples annealed at high temperatures.

For both groups of samples (low annealed and overheated) decay efficiency BLS is more rapid than for efficiency ALS. It means that lifetimes determined from the BLS decay curve are shorter compared to lifetimes determined from the ALS decay curve. Estimation of  $T_{80}$  values from the BLS and ALS results were summarized in Table 2. The apparent improvement of lifetimes in ALS results means that even unintentional illumination of samples may disrupt the proper measurements and analysis of stability.

### 3.3 Changes in Magnitude of the Light-Soaking Effect During the Aging of Solar Cell

As was mentioned, relative improvement due to the light-soaking effect is related to the quality and amount of defects in the solar-cell structure. With increasing degradation time, defects were created and the quality of solar cell decreased. In Fig. 6, the relationship between the ALS efficiency divided by the BLS efficiency and the degradation time was presented.

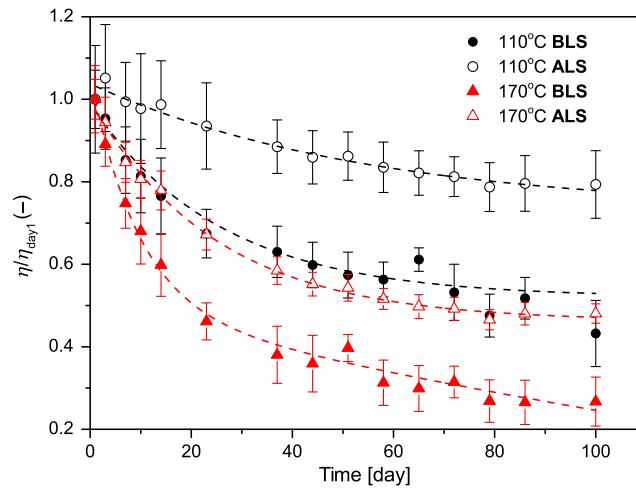


**Fig. 5** Efficiency decay for samples annealed at 110°C (black) and 170°C (red) measured before (solid circle and solid upward triangles) and after 10 min LS (open circle and open upward triangles). Each point is an average of five to six solar cells divided by average at first measurement day.

**Table 2**  $T_{80}$  values for samples annealed at various temperatures for measurement before and after LS.

Temperature of annealing (°C)	$T_{80}$ — BLS (h)	$T_{80}$ — ALS (h)
NA	336	3720
110	248	1912
130	153	1261
150	120	310
170	130	261

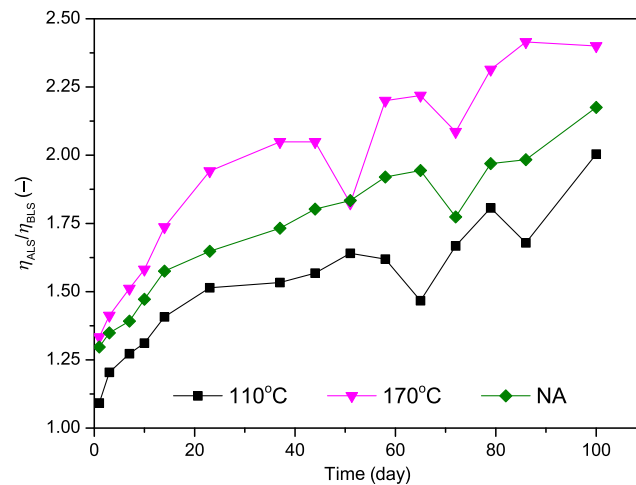


**Fig. 6** Efficiency measured after 10-min LS divided by efficiency measured before LS as a function of time for annealed at 110°C (black squares), 170°C (purple downward triangles), and for NA (green diamonds) samples. Each point is an average of five to six solar cells ALS divided by average BLS.

In the first measurement day, relative improvement of efficiency due to LS was 8% and 27% for sample annealed at 110°C and at 170°C, respectively. After 100 days, these improvements increased up to 100% and 138%, respectively. During the degradation process, trap states and defects are created due to different paths of degradation, e.g., photooxidation, diffusion of atoms, reorganization of BHJ, and many others.<sup>32–37</sup> Some of these trap states, close to the ITO/ZnO, could be filled up during the light-soaking illumination.<sup>19,22</sup> On the other hand, the trap states, close to the ZnO/P3HT:PCBM, could change the induced interfacial dipoles.<sup>23,24</sup> Presented data do not consider which interface (ITO/ZnO or ZnO/P3HT:PCBM) plays the key role in the light-soaking effect but highlight the need for taking into account the LS effect in the analysis. The impact of light-soaking effect is increasing in time and it should be considered for proper and reliable measurements and stability analysis.

### 3.4 Photodegradation Induced by Light-Soaking Measurement Procedure

Photo-induced degradation is common and well-known in P3HT:PCBM solar cells.<sup>33–35</sup> To investigate how the light-soaking effect and measurement procedure, which was applied, induce any additional photodegradation, one of the samples annealed at 130°C were measured only once in each measurement day and was not exposed to the illumination for LS. It minimized exposure of the solar cells to the light illumination and these measurements were called as never light soaked (NLS). Total illumination time under AM1.5, 1000 W/m<sup>2</sup> at the end of day #51, and  $T_{80}$  values were summarized in Table 3.

The most rapid decay of normalized efficiency curve occurred for BLS results (Fig. 7). The most flat decay was obtained for ALS measurements. A sample that was NLS was more stable, than the sample that was light soaked and was measured as BLS. It means that on the one hand LS reduces the negative impact of degradation and on the other hand LS induces the degradation of P3HT:PCBM solar cells.

### 3.5 Light Soaking and Quality of Samples

In our study, the following observation could be made: if the sample is of good quality, the light-soaking effect is weak and the light-soaking effect increases with time (degradation of sample). In Fig. 8, efficiency measured after 10-min LS versus efficiency measured before LS were presented as an average of five to six solar cells from each of five groups of samples. This figure shows all results collected in 100 days and it illustrates the light-soaking effect without degradation and time aspects.

If the sample has a high BLS efficiency, the improvement due to LS will be weaker than for the sample that has lower BLS efficiency. The better the sample is the weaker light-soaking effect could be expected, and it is independent from time and degradation aspects. In Fig. 8(a), it could be observed that the slope of the graph decreases with increasing the efficiency, and thus, the relative improvement of efficiency is decreasing with the BLS efficiency [Fig. 8(b)]. It means that for the high-efficient and defects-free devices, LS is a minor effect and it could not be observed for as-prepared devices, but it could grow in time and should be considered and analyzed in the degradation studies.

**Table 3**  $T_{80}$  values determined for measurement BLS, ALS, and NLS for solar cells annealed at 130°C.

Type of measurement	Total illumination time at the end of day #51 (min)	$T_{80}$ (h)
BLS	144	153
ALS	144	1261
NLS	1.6	341



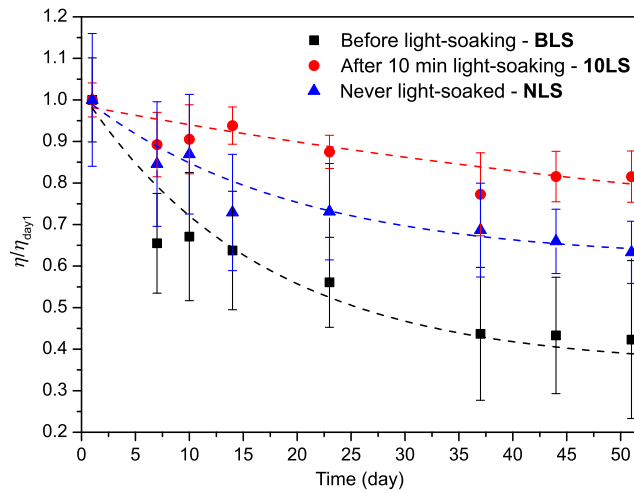


**Fig. 7** Efficiency decays for samples measured before LS (black squares), after 10 min LS (red circles), and for a sample never exposure for light-soaking illumination (blue triangles). Both groups of samples were annealed at 130°C. Each point is an average of five to six solar cells divided by average at first measurement day.

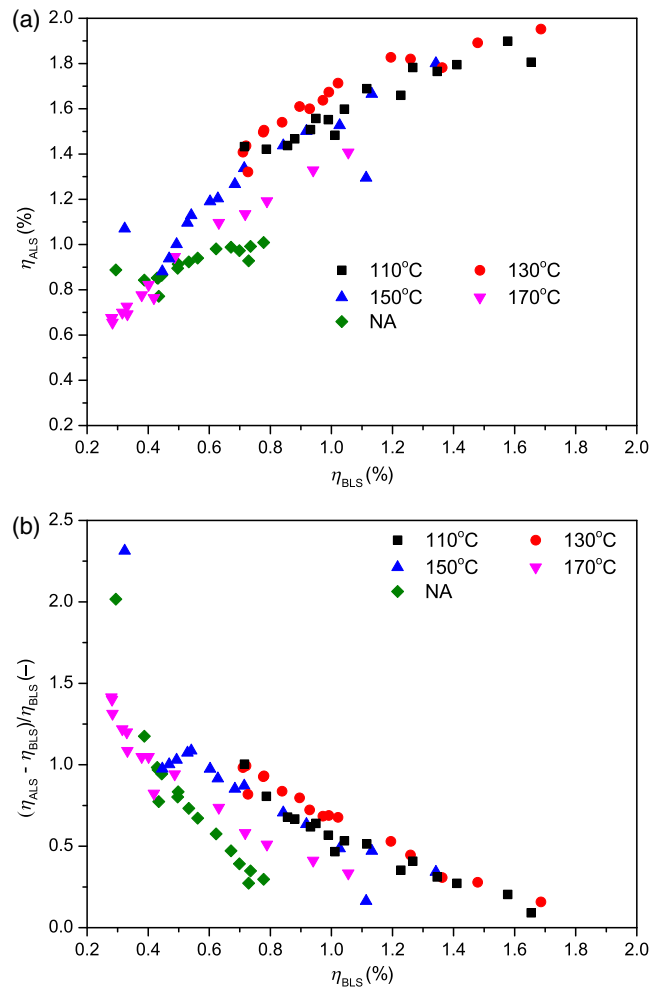


**Fig. 8** (a) Efficiency ALS as a function of efficiency BLS. (b) Relative improvement of efficiency due to LS as a function of efficiency BLS. Each point is an average of five to six solar cells.

## 4 Conclusions

Systematic investigation of the impact of light-soaking effect on the degradation studies is presented. The inverted OSCs with various qualities of active BHJ were fabricated (efficiencies in range 0.69% up to 1.86%). High temperatures of annealing (150°C and 170°C) lead to agglomeration of PCBM and, thus, low photovoltaic properties and short lifetimes compared to low temperatures of annealing (110°C and 130°C). Measurements procedure for testing the light-soaking effect was proposed, and it was conducted for 100 days. This study involved more than 30 solar-cell devices. The key issues associated with the study of stability and light-soaking effect were presented. Relatively, improvement of efficiency due to light-soaking illumination in range from 8% up to even 138% was observed. LS is changing in time and depends strongly on the quality of prepared samples. The higher the quality of the sample, the lower improvement due to LS could be expected. It means that LS for as-prepared high-efficient devices could not be observed, but after a few days/months, it could be significant. LS should be considered for reliable measurements and proper analyzing of stability data.

## Acknowledgments

The work was supported by the National Centre for Research and Development (NCBR) within the Project POSCIS under Grant No. LIDER/09/129/L-3/11/NCBR/2012).

## References

1. D. Vak et al., "Fabrication of organic bulk heterojunction solar cells by a spray deposition method for low-cost power generation," *Appl. Phys. Lett.* **91**(8), 081102 (2007).
2. E. Ahlswede et al., "Highly efficient organic solar cells with printable low-cost transparent contacts," *Appl. Phys. Lett.* **92**(14), 143307 (2008).
3. C. Lungenschmied et al., "Flexible, long-lived, large-area, organic solar cells," *Sol. Energy Mater. Sol. Cells* **91**(5), 379–384 (2006).
4. R. Søndergaard et al., "Roll-to-roll fabrication of polymer solar cells," *Mater. Today* **15**(2), 36–49 (2012).
5. T. Winkler et al., "Efficient large area semitransparent organic solar cells based on highly transparent and conductive ZTO/Ag/ZTO multilayer top electrodes," *Org. Electron.* **12**(10), 1612–1618 (2011).
6. M. Kaltenbrunner et al., "Ultrathin and lightweight organic solar cells with high flexibility," *Nat. Commun.* **3**, 770 (2012).
7. M. C. Scharber et al., "Design rules for donors in bulk-heterojunction solar cells—towards 10% energy-conversion efficiency," *Adv. Mater.* **18**, 789–794 (2006).
8. N. Yeh et al., "Organic solar cells: their developments and potentials," *Renewable Sustainable Energy Rev.* **21**, 421–431 (2013).
9. H. Hoppe et al., "Organic solar cells: an overview," *J. Mater. Res.* **19**(7), 1924–1945 (2004).
10. C. Deibel et al., "Polymer-fullerene bulk heterojunction solar cells," *Rep. Prog. Phys.* **73**(1), 096401 (2010).
11. S. Nam et al., "Inverted polymer fullerene solar cells exceeding 10% efficiency with poly(2-ethyl-2-oxazoline) nanodots on electron-collecting buffer layers," *Nat. Commun.* **6**, 8929 (2015).
12. J. A. Hauch et al., "Flexible organic P3HT:PCBM bulk-heterojunction modules with more than 1 year outdoor lifetime," *Sol. Energy Mater. Sol. Cells* **92**(7), 727–731 (2008).
13. F. C. Krebs et al., "Significant improvement of polymer solar cell stability," *Chem. Mater.* **17**(21), 5235–5237 (2005).
14. F. C. Krebs et al., "Analysis of the failure mechanism for a stable organic photovoltaic during 10 000 h of testing," *Prog. Photovoltaics Res. Appl.* **15**, 697–712 (2007).
15. F. J. Lim et al., "Influence of a novel fluorosurfactant modified PEDOT:PSS hole transport layer on the performance of inverted organic solar cells," *J. Mater. Chem.* **22**, 25057 (2012).
16. H. Kim et al., "Influence of controlled acidity of hole-collecting buffer layers on the performance and lifetime of polymer:fullerene solar cells," *J. Phys. Chem. C* **115**(27), 13502–13510 (2011).

17. K. W. Wong et al., "Blocking reactions between indium-tin oxide and poly(3, 4-ethylene dioxathiophene):poly(styrene sulphonate) with a self-assembly monolayer," *Appl. Phys. Lett.* **80**(15), 2788 (2002).
18. X.-D. Dang et al., "Morphology and conductivity modification of poly(3, 4-ethylenedioxythiophene):poly(styrene sulfonate) films induced by conductive atomic force microscopy measurements," *Appl. Phys. Lett.* **93**(24), 241911 (2008).
19. F. J. Lim et al., "Addressing the light-soaking issue in inverted organic solar cells using chemical bath deposited fluorinated TiO<sub>x</sub> electron transport layer," *J. Mater. Chem. A* **3**, 314–322 (2015).
20. H. Schmidt et al., "Transient characteristics of inverted polymer solar cells using titanium-oxide interlayers," *Appl. Phys. Lett.* **96**(24), 243305 (2010).
21. J. W. Shim et al., "Polyvinylpyrrolidone-modified indium tin oxide as an electron-collecting electrode for inverted polymer solar cells," *Appl. Phys. Lett.* **101** (7), 073303 (2012).
22. J. Kim et al., "Light-soaking issue in polymer solar cells: photoinduced energy level alignment at the sol-gel processed metal oxide and indium tin oxide interface," *J. Appl. Phys.* **111**(11), 114511 (2012).
23. T. Kuwabara et al., "Mechanistic investigation into the light soaking effect observed in inverted polymer solar cells containing chemical bath deposited titanium oxide," *J. Phys. Chem. C* **119**(10), 5274–5280 (2015).
24. S. Trost et al., "Overcoming the 'light-soaking' issue in inverted organic solar cells by the use of Al:ZnO electron extraction layers," *Adv. Energy Mater.* **3**(11), 1437–1444 (2013).
25. I. Jeon et al., "Vertical phase separation and light-soaking effect improvements by photoactive layer spin coating initiation time control in air-processed inverted organic solar cells," *Sol. Energy Mater. Sol. Cells* **140**, 335–343 (2015).
26. F. J. Lim et al., "All-in-one solar cell: stable, light-soaking free, solution processed and efficient diketopyrrolopyrrole based small molecule inverted organic solar cells," *Sol. Energy Mater. Sol. Cells* **150**, 19–31 (2016).
27. M. O. Reese et al., "Consensus stability testing protocols for organic photovoltaic materials and devices," *Sol. Energy Mater. Sol. Cells* **95**(5), 1253–1267 (2011).
28. F. C. Chen et al., "Morphological study of P3HT:PCBM blend films prepared through solvent annealing for solar cell applications," *Sol. Energy Mater. Sol. Cells* **94**(12), 2426–2430 (2010).
29. L. Chang et al., "Effect of trace solvent on the morphology of P3HT:PCBM bulk heterojunction solar cell," *Adv. Funct. Mater.* **21**(11), 1779–1787 (2011).
30. H. Hoppe et al., "Morphology of polymer/fullerene bulk heterojunction solar cells," *J. Mater. Chem.* **16**, 45–61 (2006).
31. M. Basta et al., "Method to analyze the ability of bulk heterojunctions of organic and hybrid solar cells to dissociate photogenerated excitons and collect free carriers," *J. Appl. Phys.* **115** (17), 174504 (2014).
32. D. Chen et al., "P3HT/PCBM bulk heterojunction organic photovoltaics: correlating efficiency and morphology," *Nano Lett.* **11**(2), 561–567 (2011).
33. M. Jørgensen et al., "Stability/degradation of polymer solar cells," *Sol. Energy Mater. Sol. Cells* **92**(3), 686–714 (2008).
34. S. Karuthedath et al., "The effect of oxygen induced degradation on charge carrier dynamics in P3HT:PCBM and Si-PCPDTBT:PCBM thin films and solar cells," *J. Mater. Chem. A* **3**, 3399–3408 (2015).
35. M. O. Reese et al., "Photoinduced degradation of polymer and polymer-fullerene active layers: experiment and theory," *Adv. Funct. Mater.* **20**(20), 3476–3483 (2010).
36. A. Tournebize et al., "New insights into the mechanisms of photodegradation/stabilization of P3HT:PCBM active layers using Poly(3-hexyl - d13 -Thiophene)," *Chem. Mater.* **25**(22), 4522–4528 (2013).
37. S. S. Ghosh et al., "Organic solar cells based on acceptor-functionalized diketopyrrolopyrrole derivatives," *J. Photonics Energy* **5**(1), 057215 (2015).

**Michał Dusza** graduated from Wrocław University of Technology, Faculty of Microsystem Electronics and Photonics. He is a PhD student at the Institute of Low Temperatures and

Structure Research, PAS, in Wrocław. His research activity focuses on novel materials for optoelectronic devices, especially for organic and perovskite solar cells, starting with processing technologies up to complex characterization and modeling of materials and devices. He is a Management Committee Substitute Poland in COST MP1307 action.

**Wiesław Strek** works at the Institute of Low Temperatures and Structure Research, PAS, in Wrocław. His research activity covers laser spectroscopy, luminescence properties of rare earth, glasses and nanostructures, nonlinear optics, laser-matter interaction, nanophosphors, nanoceramics, optical sensors. He is a member of the editorial boards of *Journal of Alloys and Compounds*, *Journal of Rare Earth*, *Reports in Physics*, and *Polish Materials Science*. He is a author/coauthor of more than 450 papers, more than 5000 citations, Hirsch index-34. He is cocreator more than 30 patents and patent applications.

**Filip Granek** received his MSc degree in electrical engineering from Wrocław University of Technology, Poland, in 2004, and a PhD degree engineering physics from Albert Ludwigs University of Freiburg, Germany, in 2009. His research focus includes novel materials and processing technologies for optoelectronics devices and printed electronics. Since 2015 he has been CTO of XTPL company. He has published 70 technical papers and is inventor of 15 international patents and patent applications.